Field-effect modulation of contact resistance between carbon nanotubes

Yoshihiro Kodama,[a] Ryota Sato, Nobuhito Inami, Eiji Shikoh, Yoshiyuki Yamamoto, and Hidenobu Hori
School of Materials Science, Japan Advanced Institute of Science and Technology (JAIST), 1-1 Asahidai, Nomi, Ishikawa 923-1292, Japan

Hiromichi Kataura
Nanotechnology Research Institute, National Institute of Advanced Industrial Science and Technology (AIST), Central 4, 1-1 Higashi, Tsukuba, Ibaraki 305-8562, Japan

Akihiko Fujiwara[a]
School of Materials Science, Japan Advanced Institute of Science and Technology (JAIST), 1-1 Asahidai, Nomi, Ishikawa 923-1292, Japan

(Received 3 July 2007; accepted 10 September 2007; published online 28 September 2007)

Local transport properties of a carbon nanotube (CNT) thin-film transistor (TFT) have been investigated by conducting atomic force microscopy. The current in a CNT bundle is almost constant, whereas it drastically decreases at the contacts between CNTs. Current drops at the contacts are reduced with increasing negative gate voltage V_G. The results show that the contact resistance between CNTs can be modified by V_G, and the operation of CNT-TFT is mainly governed by the modulation of contact resistance. © *2007 American Institute of Physics*.
[DOI: 10.1063/1.2790805]

Carbon nanotubes (CNTs) have attracted great attention as potential materials for electronic devices because of their one-dimensional structure and tubular honeycomb network in the nanometer scale.[1] They can be either metallic or semiconducting, depending on the chirality and diameter of the CNTs.[2–5] Findings of many kinds of functions, such as single electron transport,[6,7] quantum magnetic transport,[8,9] spin coherent transport,[10] and photoconductivity,[11] were also reported, and have stimulated both fundamental research and practical applications of CNTs. For the application of CNTs to semiconductor devices, there are two prominent but different streams; one is the development of high-performance molecular devices and another is that of low-cost large-area devices. A field-effect transistor (FET) using an individual CNT as the channel is a typical example of the former case. Owing to its simple device structure, it has been clarified that an individual CNT FET is operated by modulation of Schottky barrier at the contacts between CNT and source/drain electrodes.[12,13] Although logic circuits were fabricated by integrating individual CNT FETs,[14] circuit performance is not yet as high enough as expected, in spite of the high carrier mobility of CNTs. One of the reasons is a limit of current-carrying capacity of individual CNTs.[15] In order to improve circuit performance, many approaches are currently being tested.

Since the development of a thin-film transistor (TFT) using a randomly networked film of CNTs as a channel,[15] much research on the fabrication of transparent and flexible devices has been performed. Advantages of the use of CNTs for transparent and flexible TFTs are the high aspect ratio, mechanical strength, and flexibility of CNTs. In addition, there is no limit of current-carrying capacity in CNT-TFTs unlike in individual CNT FETs.[15] In spite of the great progress in the development of CNT-TFTs,[16,17] the detailed mechanism of device operation of CNT-TFTs has not been clarified. Characterization of CNT-TFTs is very complicated because of the complex current paths in randomly networked CNT thin films. This situation is completely different from that of individual CNT FETs. It is well known that the transport properties of randomly networked CNT thin films are affected by parasitic resistance, such as contact resistance between CNTs. Although possible models, such as variable-range hopping[18] (VRH) and fluctuation-induced tunneling[19] (FIT) are proposed,[20] the origin of parasitic resistance is not fully understood. Therefore, understanding of device characteristics of CNT-TFTs is very important, not only for practical applications in transparent and flexible devices using CNTs, but also for fundamental research on transport properties between molecules. In this work, we investigated local transport properties of CNT-TFTs by means of atomic force microscope (AFM) with conducting tip. We will discuss the field effect on the carrier transport between CNT molecules.

CNT-TFTs were fabricated by a simple solution process.[21] A heavily doped *n*-type silicon wafer with 400 nm thickness of thermally oxidized SiO_2 layer on the surface was used as substrate. The drain electrode was patterned on an insulating SiO_2 layer, using an electron beam lithography method. Au was deposited using dc sputtering (Elionix ESC-101) at a deposition rate of about 0.1 nm/s. The thickness of drain electrodes was 300 nm. The doped silicon layer of the wafer was used as a gate electrode. The single-wall CNTs (SWCNTs) were synthesized by laser ablation using Fe/Co as catalytic metals at the furnace temperature of 900 °C. The mean diameter of the SWCNTs (d) was determined to be about 1.4 nm from the Raman frequency of the radial breathing mode (ω_{RBM}) with the known equation d (nm) $=248/\omega_{RBM}$ (cm^{-1}).[22] The SWCNTs were purified with H_2O_2, HCl, and NaOH. The details of the synthesis and the purification procedures have been published previously.[23] The SWCNTs form bundles by van der Waals interaction, and those bundles aggregate together. Purified SWCNTs were dispersed in ethanol and were ultrasonicated for 3 days

[a]Present address: Toppan Printing Co., Ltd.

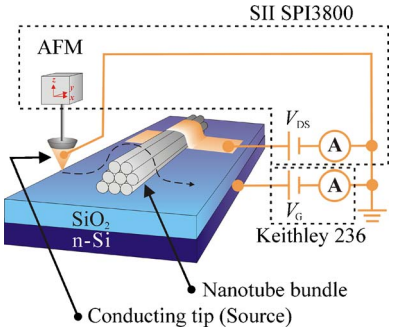

FIG. 1. (Color online) Schematic of local current measurements by using the AFM with conducting tip.

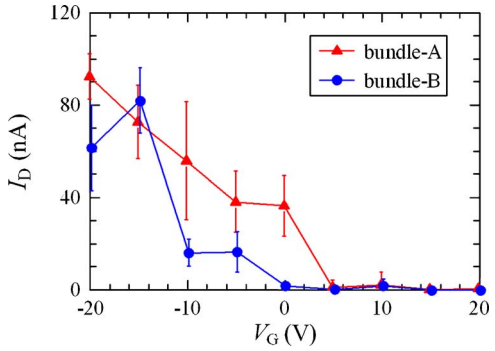

FIG. 3. (Color online) V_G dependence of averaged current at the bundles A and B.

in order to disperse to individual bundles. Dispersion of CNTs in ethanol was dropped near the drain electrode on the substrate, and N_2 was blown to dry up the ethanol. After this series of treatments, no significant damage of CNTs was observed by Raman scattering and AFM measurements. Local transport properties were measured by means of a conducting AFM method.[24–26] A conducting AFM tip (SII SN-AF01-A) was used as a mobile source electrode. A schematic of the measurement setup is shown in Fig. 1. Application of drain-source voltage V_{DS} and detection of drain current I_D were performed using internal circuit of measurement system (SII SPI3800) for scanning tunneling microscopy. V_{DS} was set to be 0.05 V. Gate voltage V_G was applied by an external source-measure unit (Keithley 236). All measurements were performed by contact mode at room temperature in air.

Figure 2 shows a topological AFM image and local current images of a CNT-TFT at three different V_G's. The fine lines depict CNT bundles, and the lower part of each image is the drain electrode of Au. From the height of individual bundles in the topological image [Fig. 2(a)], the diameters of bundles are distributed about 8–30 nm, showing that each bundle consists of 20–300 CNTs. Here, we focus on the current path from the drain electrode through bundle A and bundle B to the source electrode (AFM tip). Clear gate voltage dependence of local current at bundles A and B was observed, as shown in Figs. 2(b)–2(d). Current values increase with decreasing V_G. This characteristic is consistent with *p*-type operation of CNT-TFT. It is important to note that the local current on the electrode of Au was very low. This can be attributed to surface oxidation and/or the residue on the surface because current increases by repetitious measurements. This phenomenon was not observed for SWCNTs. The result shows that the surface of SWCNTs is hardly smeared, and that it is very clean even in an ambient environment. This is one of the significant features of SWCNTs for application to electronic devices.

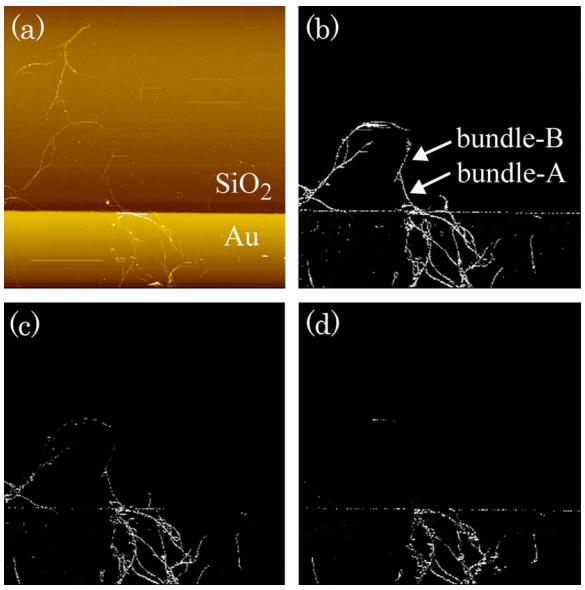

FIG. 2. (Color online) AFM images of a CNT-TFT near the drain electrode. (a) Topological AFM image. Local current images for (b) $V_G=-20$ V, (c) $V_G=0$ V, and (d) $V_G=20$ V. The size of images is 20×20 μm^2. Current values are shown by gradation: black and white correspond to 0 and 100 nA, respectively. Scale is not linear, and halftone (50% gray) corresponds to 5 nA.

Spatial variation of detected local current through a conducting AFM tip corresponds to the variation of local resistance. For $V_G=-20$ V [Fig. 2(b)], high values of current were observed in both bundles A and B. On the other hand, for $V_G=20$ V [Fig. 2(d)], current almost vanished in both bundles A and B. For $V_G=0$ V [Fig. 2(c)], however, current value drastically decreases mainly at the contact between bundles A and B, whereas current in a CNT bundle is almost constant for each bundle. In this measurement method, current decreases drastically at the high resistance position, whereas it shows a constant value at the low resistance area. This result shows that resistance in the bundle is negligible, and most of the resistance in the current path is located at the contact between CNT bundles. This result is consistent with our previous report on local transport properties of CNT junction without application of V_G.[25] It is well known [from the investigation of the individual CNT FETs (Refs. 12 and 13)] that the contact resistance between metal electrodes and CNTs decreases with application of V_G. Increase in current of bundle A, which is connected to the drain electrode, with decreasing V_G can be explained by this scenario. On the other hand, increase in current of bundle B can be attributed to the decrease in contact resistance between bundles A and B.

Figure 3 shows V_G dependence of averaged current at bundles A and B. Data were estimated from the average of ten highest values in each bundle. Actually, V_G dependence of current observed at bundle B is different from that at bundle A, which is consistent with the above discussion. The current of bundle B shows negligible values down to $V_G=0$ V, and current increases for $V_G<0$ V, whereas current of bundle A begins to increase at $V_G=5$ V and shows a finite value at $V_G=0$ V. This result shows that the contact resistance between bundles A and B dominates the total resistance

for $0\ \mathrm{V} \leqslant V_G \leqslant 5\ \mathrm{V}$, and begins to decrease at $V_G = 0$ V with decreasing V_G. Increase of uniform current in bundles is attributed to the decrease of resistance at the contacts. For $V_G \leqslant -5$ V, contact resistance becomes negligible or vanishes. From this result, we can conclude that CNT-TFT device is operated by a modulation of contact resistance using V_G because most of the resistance in the current path is located at the contacts.

Finally, we discuss the mechanism of electron transport through contact between CNTs. There are two possible models, VRH and FIT, as mentioned above. The result in this work that the contact resistance decrease with the application of negative V_G can be explained by the reduction of activation energy through the carrier accumulation: both models can account for this. However, the negligible contact resistance for $V_G \leqslant -5$ V cannot be explained by the FIT model because large enhancement of tunneling probability by the application of V_G cannot be expected. Therefore, we propose the VRH as the mechanism of electron transport through contact between CNTs. Our experimental technique in this work gives us information on the local real-space distribution of carriers and complements the characterization based on the overall output characteristics of devices. Carrier transport between bundles discussed in this letter may be related to that between grains in organic materials, and higher resolution measurements will clarify the carrier transport among molecules in real space.

In summary, we have demonstrated local transport measurements on CNT-TFTs by means of AFM with conducting tip. Our experiments revealed that the contact resistance between CNT bundles can be modified by V_G, and the operation of CNT-TFT is governed by the modulation of contact resistance. It can be expected that the conducting AFM technique presented in this work will clarify mechanisms of inter- and intramolecule carrier transport of molecular devices and organic materials.

This work is supported in part by the Grant-in-Aid for Scientific Research (Grant Nos. 16206001 and 17540322) from the Ministry of Education, Culture, Sports, Science and Technology (MEXT) of Japan, and a NEDO Grant (Grant No. 04IT5) from the New Energy and Industrial Technology Development Organization (NEDO).

[1] S. Iijima, Nature (London) **354**, 56 (1991).
[2] R. Saito, M. Fujita, G. Dresselhaus, and M. S. Dresselhaus, Appl. Phys. Lett. **60**, 2204 (1992).
[3] R. Saito, M. Fujita, G. Dresselhaus, and M. S. Dresselhaus, Phys. Rev. B **46**, 1804 (1992).
[4] N. Hamada, S. Sawada, and A. Oshiyama, Phys. Rev. Lett. **68**, 1579 (1992).
[5] H. Ajiki and T. Ando, J. Phys. Soc. Jpn. **62**, 1255 (1993).
[6] S. J. Tans, M. H. Devoret, H. Dai, A. Thess, R. E. Smalley, L. J. Geerligs, and C. Dekker, Nature (London) **386**, 474 (1997).
[7] M. Bockrath, D. H. Cobden, P. L. McEuen, N. G. Chopra, A. Zettl, A. Thess, and R. E. Smalley, Science **275**, 1922 (1997).
[8] A. Bachtold, C. Strunk, J.-P. Salvetat, J.-M. Bonard, L. Forro, T. Nussbaumer, and C. Schönenberger, Nature (London) **397**, 673 (1999).
[9] A. Fujiwara, K. Tomiyama, H. Suematsu, M. Yumura, and K. Uchida, Phys. Rev. B **60**, 13492 (1999).
[10] K. Tsukagoshi, B. W. Alphenaar, and H. Ago, Nature (London) **401**, 572 (1999).
[11] A. Fujiwara, Y. Matsuoka, H. Suematsu, N. Ogawa, K. Miyano, H. Kataura, Y. Maniwa, S. Suzuki, and Y. Achiba, Jpn. J. Appl. Phys., Part 2 **40**, L1229 (2001).
[12] M. Freitag, M. Radosavljevic, Y. Zhou, A. T. Johnson, and W. F. Smith, Appl. Phys. Lett. **79**, 3326 (2001).
[13] S. Heinze, J. Tersoff, R. Martel, V. Derycke, J. Appenzeller, and Ph. Avouris, Phys. Rev. Lett. **89**, 106801 (2002).
[14] A. Bachtold, P. Hadley, T. Nakanishi, and C. Dekker, Science **294**, 1317 (2001).
[15] E. S. Snow, J. P. Novak, P. M. Campbell, and D. Park, Appl. Phys. Lett. **82**, 2145 (2003).
[16] S.-H. Hur, O. O. Park, and J. A. Rogers, Appl. Phys. Lett. **86**, 243502 (2005).
[17] T. Takenobu, T. Takahashi, T. Kanbara, K. Tsukagoshi, Y. Aoyagi, and Y. Iwasa, Appl. Phys. Lett. **88**, 033511 (2006).
[18] N. F. Mott and E. A. Davis, *Electronic Processes in Non-Crystalline Materials* (Clarendon, Oxford, 1979).
[19] P. Sheng, Phys. Rev. B **21**, 2180 (1980).
[20] E. Kymakis and G. A. J. Amaratunga, J. Appl. Phys. **99**, 084302 (2006).
[21] M. Shiraishi, T. Takenobu, T. Iwai, Y. Iwasa, H. Kataura, and M. Ata, Chem. Phys. Lett. **394**, 110 (2004).
[22] M. S. Dresselhaus, G. Dresselhaus, R. Saito, and A. Jorio, Phys. Rep. **409**, 47 (2005).
[23] H. Kataura, Y. Maniwa, T. Kodama, K. Kikuchi, K. Hirahara, K. Suenaga, S. Iijima, S. Suzuki, Y. Achiba, and W. Kratschmer, Synth. Met. **121**, 1195 (2001).
[24] A. Fujiwara, R. Iijima, K. Ishii, H. Suematsu, H. Kataura, Y. Maniwa, S. Suzuki, and Y. Achiba, Appl. Phys. Lett. **80**, 1993 (2002).
[25] A. Fujiwara, R. Iijima, H. Suematsu, H. Kataura, Y. Maniwa, S. Suzuki, and Y. Achiba, Physica B **323**, 227 (2002).
[26] Y. Yaish, J.-Y. Park, S. Rosenblatt, V. Sazonova, M. Brink, and P. L. McEuen, Phys. Rev. Lett. **92**, 046401 (2004).